by forest expansion or afforestation with pines and eucalypts. Secondary grasslands, formed after deforestation or removal of plantations, have completely different species compositions from primary grasslands (*4*, *6*). Forbs with USOs and underground trees are particularly vulnerable, with no recovery to old-growth conditions after decades of natural succession.

These studies are revealing striking differences in old-growth versus secondary grasslands. However, the scale of analysis does not yet permit large-scale identification of old-growth grasslands. It is not yet possible to map old-growth grasslands at the scale of the WRI Atlas of Forest and Landscape Restoration Opportunities (*1*–*3*). The Food and Agriculture Organization (FAO) uses tree cover and height to classify forest and ignores the herbaceous layer (*5*). Yet there are profound functional differences between open woodlands with a highly flammable grassy understorey and closed forests that lack fuel to burn. Ultimately, old-growth versus secondary grasslands will have to be classified by identifying characteristics of the herbaceous layer, such as grass composition, that are visible from satellites and that are also proxies for primary grasslands.

There are many fundamental unanswered questions about grassy biomes, their function, origins, and antiquity. The recent spate of papers on these fascinating systems suggests that this neglect is coming to an end. There has been considerable progress in identifying old-growth grasslands and their ecological requirements, and this bodes well for restoring forests and the services they provide while also maintaining ancient tropical grassy ecosystems. It would be a travesty if ancient grasslands are replaced by ill-conceived forest plantation projects because of misconceptions about the origins of tropical grassy systems. ■

REFERENCES

1. World Resources Institute maps; www.wri.org/resources/maps/.
2. L. Laestadius *et al.*, *Unasylva* **238**, 47 (2011).
3. J. W. Veldman *et al.*, *BioScience* **65**, 1011 (2015).
4. W. J. Bond, C. L. Parr, *Biol. Cons.* **143**, 2395 (2010).
5. C. L. Parr *et al.*, *TREE* **29**, 205 (2014).
6. J. W. Veldman *et al.*, *Front. Ecol. Env.* **13**, 154 (2015).
7. R. B. Jackson *et al.*, *Environ. Res. Lett.* **3**, 044006 (2008).
8. C. Nogueira *et al.*, *J. Biogeog.* **38**, 1907 (2011).
9. G. E. Overbeck *et al.*, *Persp. Plant Ecol. Evol. Syst.* **9**, 101 (2007).
10. R. F. Noss, *Forgotten Grasslands of the South: Natural History and Conservation* (Island Press, 2012).
11. R. F. Noss *et al.*, *Div. Distr.* **21**, 236 (2015).
12. M. S. Vorontsova, S. E. Rakotoarisoa, *Malagasy Nature* **8**, 14 (2014).
13. M. F. Simon *et al.*, *Proc. Natl. Acad. Sci.* **106**, 20359 (2009).
14. F. White, *Gardens Bull. Singapore* **24**, 57 (1976).
15. O. Maurin *et al.*, *New Phyt.* **204**, 201 (2014).
16. S. Scheiter *et al.*, *New Phyt.* **195**, 653 (2012).

10.1126/science.aad5132

GEOCHEMISTRY

Lower-mantle materials under pressure

Laboratory measurements provide a window into Earth's mantle dynamics

By **Jiuhua Chen**

Modern high-pressure experimental techniques have enabled us to achieve the pressure and temperature at the center of Earth (about 360 GPa and 6000 K) in laboratories. However, studies of rheological properties of minerals under controlled strain rate (creep experiments) have been limited to the pressure equivalent to that in Earth's transition zone, a depth only about one-tenth of Earth's radius. Determinations of rheological laws that govern the flows and viscosities of minerals in Earth's deep mantle have been far beyond our reach. In the absence of such critical data, the nature of mantle dynamics—such as whether the convection involves the entire lower mantle, yielding a chemically homogeneous deep mantle—remains controversial. Discovery of the breakdown of ringwoodite into the denser bridgmanite and magnesiowüstite phases at 24 GPa (*1*) removed the need for a major chemical discontinuity in Earth inferred from observations of a strong seismic reflector at 660 km depth. On page 144 of this issue, Girard *et al.* (*2*) report on the detailed rheological nature of this bridgmanite plus magnesiowüstite mineral aggregate, shedding more light on the mantle convection. The integration of brilliant synchrotron radiations and rotating apposed anvils enables creep experiments for large strain at pressures equivalent to that in Earth's lower mantle.

> ***"All the evidence leads us to a hybrid convection model—a mixture of layered and whole-mantle circulations."***

Center for High Pressure Science and Technology Advanced Research, Jilin University, Changchun 130015, China, and Center for the Study of Matter at Extreme Conditions, Department of Mechanical and Materials Engineering, Florida International University, Miami, FL 33199, USA. E-mail: chenj@fiu.edu

Nearly 90% of the lower mantle is occupied by the minerals bridgmanite and magnesiowüstite. Bridgmanite is believed to be the rheologically strongest phase at high pressure and high temperature among all dominant minerals in the shallower mantle (*3*), giving rise to a high viscosity of the lower mantle relative to the upper mantle and the transition zone. In their creep experiment on these two minerals directly converted from natural olivine, Girard *et al.* not only recognized that bridgmanite is substantially stronger than magnesiowüstite and that a large fraction of the strain is accommodated by magnesiowüstite, but also observed a tendency of strain weakening of bridgmanite when large strain (>40%) is applied. These observations may indicate shear localizations in the lower mantle—a result that would have an impact on the mantle dynamics.

If we assume that large enough strains occurring in deep mantle convection eventually produce interlinking of the weak magnesiowüstite phase in the microstructure of the mineral aggregate due to the shear localization, then a transition of its rheological behavior from a load-bearing framework (LBF) phase to an interconnected weak layers (IWL) phase might be expected on the basis of the semitheoretical model described by Handy (*4*). Taking 2×10^{21} Pa·s and 1×10^{19} Pa·s as the viscosities of bridgmanite and magnesiowüstite, respectively, at the top of the lower mantle (*5*), the viscosities of the mineral aggregate for the IWL and LBF regions would be 4.5×10^{19} Pa·s and 1.5×10^{21} Pa·s, respectively (assuming a bridgmanite/magnesiowüstite volume ratio of 7:2). This contrast in viscosity, as a result of shear localization, provides us with key information about the lower mantle such as long-lived geochemical reservoirs and the absence of seismic anisotropy in the majority of the lower mantle. The result may actually have much broader implications for our understanding of the lower mantle.

High viscosity of the lower mantle is considered to be the major resistance slowing down the sinking rate of a subducting slab (*6*). This is true at the early stage of convec-

tion, when the lower mantle is in the LBF state. Once the downwelling process triggers shear localization around the sinking slab, however, the lower viscosity of the IWL zone formed along the slab will promote the subduction to a much faster rate. The subduction history of the Tethyan region (*7*) reveals free sinking rates of about 3 cm/year in the upper mantle and 2 cm/year in the lower mantle, corresponding to only a factor of 5 difference in viscosity. This is remarkably consistent with the estimated weakening of the shear localization if the bulk viscosities of the upper and lower mantles differ by two orders of magnitude.

Whether mantle convection occurs through layered circulations (favored by geochemical observations) or through a whole-mantle circulation (preferred by geodynamic modeling) is unclear. Viscosity profiling derived from oceanic geoid and seismic tomography indicates a low-viscosity zone at the top of the lower mantle (*8*). A large amount of strain caused by lateral flow at the top of the lower mantle may induce such a low-viscosity layer. Joint inversion of long-wavelength mantle convection and postglacial rebound data (*9*) reveals a viscosity contrast of 1.5 orders of magnitude between the low-viscosity layer and the mantle beneath, matching that expected from the shear localization. Although stratified convections are acceptable to geodynamic modeling, the origin of the low-viscosity layer on the top of the lower mantle is unclear (*10*). The rheological property of the lower-mantle mineral assemblage lays an important foundation in terms of mineral physics for such layered convection within the lower mantle. In addition, a three-dimensional radially anisotropic model of shear velocity (*11*) indicates that the lower mantle is more anisotropic at the top and bottom, signifying flow-induced shape or lattice-preferred orientation in these regions. Nonetheless, a purely layered mantle convection model is insufficient for the heat removal from Earth's interior. High-resolution seismic imaging indicates that some subduction slabs deflect at the base of the transition zone and some reach the bottom of the lower mantle. All the evidence leads us to a hybrid convection model—a mixture of layered and whole-mantle circulations (see the figure).

The work by Girard *et al.* is a breakthrough in high-pressure creep experiment technique. The result on the rheological property of bridgmanite and magnesiowüstite aggregate offers critical experimental data of mineral physics helping us to illustrate many observations and models in geodynamics, geochemistry, and geophysics, although the consequential promoted subduction and reduced viscosity in the IWL zone along the slabs do not seem to support the cessation of earthquakes in the lower mantle. Some other facts, such as temperature sensitivity of strength required for runaway instability in the mantle-dominant minerals (*12*), may have to be considered to explain this deep seismicity phenomenon. ■

REFERENCES

1. E. Knittle, R. Jeanloz, *Science* **235**, 668 (1987).
2. J. Girard, G. Amulele, R. Farla, A. Mohiuddin, S.-i. Karato, *Science* **351**, 144 (2016).
3. J. Chen, D. J. Weidner, M. T. Vaughan, *Nature* **419**, 824 (2002).
4. M. R. Handy, *J. Struct. Geol.* **16**, 287 (1994).
5. D. Yamazaki, S.-i. Karato, *Am. Mineral.* **86**, 385 (2001).
6. G. Stadler *et al.*, *Science* **329**, 1033 (2010).
7. E. Hafkenscheid, M. J. R. Wortel, W. Spakman, *J. Geophys. Res.* **111**, B08401 (2006).
8. M. Kido, D. A. Yuen, O. Čadek, T. Nakakuki, *Phys. Earth Planet. Inter.* **107**, 307 (1998).
9. A. M. Forte, J. X. Mitrovica, *Geophys. Res. Lett.* **23**, 1147 (1996).
10. L. Wen, D. L. Anderson, *Earth Planet. Sci. Lett.* **146**, 367 (1997).
11. M. Panning, B. Romanowicz, *Geophys. J. Int.* **167**, 361 (2006).
12. J. Chen, *J. Phys. Chem. Solids* **71**, 1032 (2010).

10.1126/science.aad7813

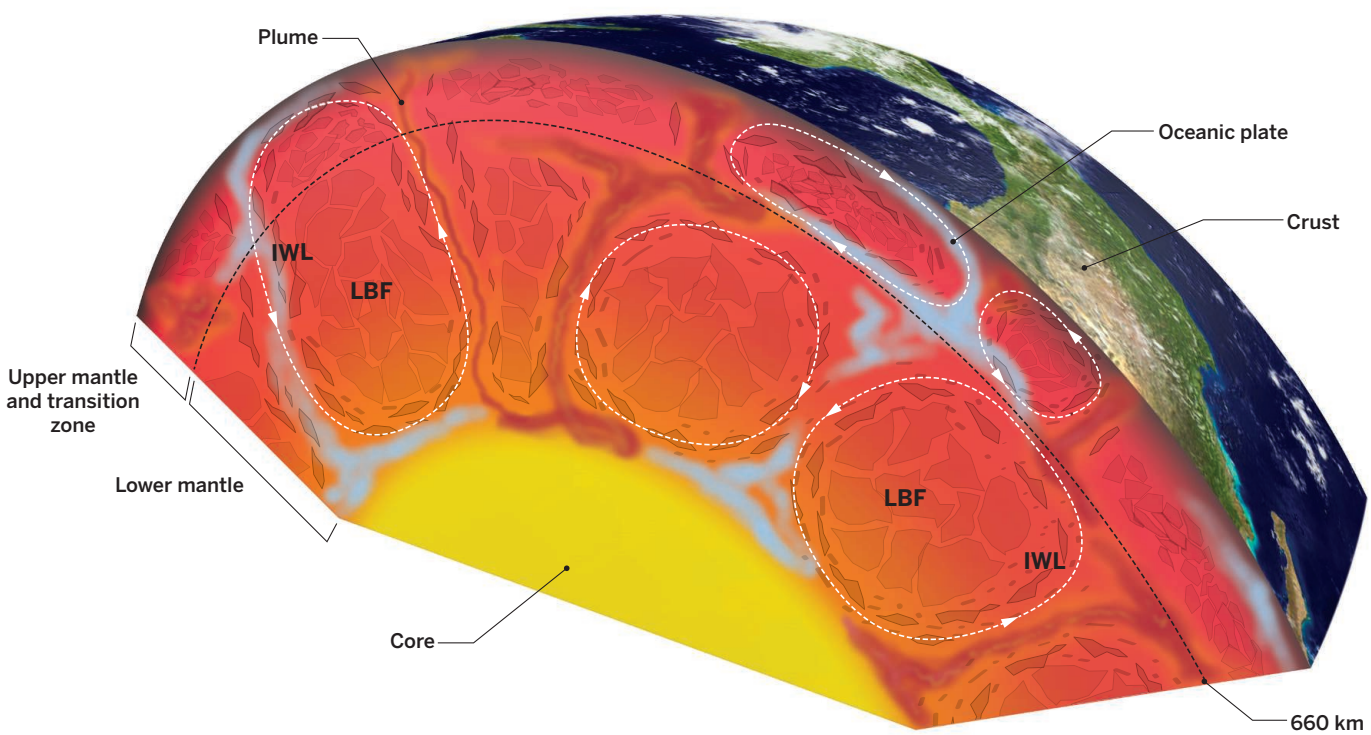

ILLUSTRATION: C. BICKEL/*SCIENCE*

Hybrid mantle convection model. Subducting slabs bring oceanic plates (blue) into the deep mantle. The slabs deflected at the 660-km discontinuity form layered convection within upper mantle and transition zone. The slabs penetrating into the lower mantle reaching the core-mantle boundary form whole-mantle convection. Plumes (red) rise from the core-mantle boundary, bringing materials that are enriched in incompatible elements relative to the expected mantle average back to the 660-km discontinuity. Some of them penetrate through the discontinuity, whereas others are deflected and may produce secondary upper-mantle plumes. Shear localization induces interconnected weak layers (IWL) along the slabs or plumes as well as the top and bottom of the lower mantle, yielding a less efficient mixing for the central LBF (load-bearing framework) part of the lower mantle (the reason for long-lived geochemical reservoirs).